

# Approximate analysis of the diffraction efficiency of transmission phase holographic gratings with smooth non-sinusoidal relief

ION ANDRIES<sup>a\*</sup>, TIGRAN GALSTIAN<sup>b</sup>, ARCADI CHIRITA<sup>c</sup>

<sup>a</sup>*Department of Mathematics and Informatics, Moldova State University, Chisinau, Republic of Moldova*

<sup>b</sup>*Faculty of Science and Engineering, Laval University, Quebec, Canada*

<sup>c</sup>*Department of Physics and Engineering, Moldova State University, Chisinau, Republic of Moldova*

In the article is presented the electro-dynamic model and method for numerical analysis of the diffraction efficiency of thin holographic diffraction gratings. Self-developing holographic gratings are easy to fabricate and can provide relatively high diffraction efficiency. Some photosensitive materials, such as chalcogenide glassy semiconductors of doped As-S-Se-Sn system used in a photo-thermoplastic recording process demonstrate the ability of registration the relief-phase gratings with efficiency up to 40% in transmitted light. The efficiency is highly dependent on the grating profile shape (groove shape and depth). Theoretical analysis is performed using the method of spectral expansions for periodic lattices. Semi-analytical dependences of efficiency on parameters of lattices with arbitrary continuous profile, including experimentally measured one by AFM, are obtained. They allow without using cumbersome numerical calculations to obtain the optimal shape of the lattice profile with maximum efficiency in a given diffraction order. A satisfactory agreement between numerical calculations and experimental measurements is demonstrated. It is shown that the optimal shape of the lattice for maximum efficiency tends to that of a symmetrical binary grating for which the theoretical limiting value of efficiency is 40.5%.

(Received February 05, 2015; accepted February 10, 2016)

*Keywords:* Holographic gratings, Non-sinusoidal profile, Diffraction efficiency, Photo-thermoplastic carriers, Numerical analysis

## 1. Introduction

Self-developing holographic diffraction gratings are easy to fabricate and can provide relatively high diffraction efficiency (DE). They are produced in the process of registration of the interference field of two coherent laser beams falling at angles of  $\alpha$  and  $\beta$  to the plane of recording material. At this, the grating's period in general form can be written as

$$d = \frac{\lambda}{n \cdot |\sin \alpha \pm \sin \beta|}, \quad (1)$$

where  $\lambda$  – wavelength in the vacuum,  $n$  – average refractive index of the medium in which the lattice is recorded. The sign "+" corresponds to angles of incidence, measured on opposite sides of the normal, and the sign "-" – to angles, measured on one side of this normal.

In the simplest case the structure of the recorded grating has a sinusoidal form. The theoretical limit of the "thin" sinusoidal grating's DE is 33.9% [1-3]. A sinusoidal diffraction grating is the simplest periodic structure that can be recorded on a photosensitive material. However, the holographic gratings with smooth, close to sinusoidal, profile may be achieved only in case of linear response of the recording media. In practice, the non-linear response of the material can provide modulation of surfaces, which are drastically different from the sinusoidal form. Experiments

show [4] that, in case of non-sinusoidal profile, the first-order DE of gratings can reach 40% in transmitted light. In this case the efficiency is highly dependent upon the shape of the grating profile (groove's shape and depth). Understanding of the importance of those parameters and of their control is thus crucial for obtaining gratings with highest efficiency.

A big variety of recording processes and materials is used in the manufacture of holographic diffraction gratings, including recording on photochromics, photopolymers, photoresists, photo-thermoplastics and other photosensitive materials. As well, the gratings may be of different kind, such as surface-relief phase gratings or volume planar gratings with bulk refractive index or conductivity modulation. Selected papers related to holographic recording materials and their processing methods are presented in the well known SPIE Milestone volume [5]. Numerous studies [6-8], including ours [9-13], have shown that extremely high DE values for holographic diffraction gratings may be achieved using the photo-thermoplastic (PTP) recording method. The PTP method is physically reduced to the creation of the light modulated mechanical relief on the surface of a thermoplastic layer. Due to the "amplification" of the modulation rate by an additionally applied electric field, its effective photosensitivity is very high. So, it can reach values of  $\sim 10^6 \text{ cm}^2\text{J}^{-1}$  for some of PTP recording media [12] based on chalcogenide glassy semiconductors of doped As-S-Se-Sn system and polymeric thermoplastic materials with

optimal deformation characteristics, synthesized from different copolymers of N-vinylcarbazole group. Also, the resolution of such PTP materials is relatively high and for some recording conditions may reach  $4000 \text{ mm}^{-1}$ . Under those conditions the PTP carriers have the ability of registration of relief-phase gratings with high value of DE. It is important to emphasize that the high values of the individual registration characteristics from their full set can be obtained simultaneously, on one and the same sample [11]. Taking into account that the fabrication process of holographic gratings is quite quick and low cost, it makes PTP carriers the most suitable for real-time hologram interferometry and high-speed signal processing.

High dependence of DE on the grating profile shape as well as on the electro-optical properties of the grating's material opens the future prospects to improve the diffraction characteristics of PTP carriers by controlling these characteristics. Therefore the basic problem is to describe accurately the properties of the diffraction gratings of different kind. Several theoretical models and methods have been proposed for it [14-23]. The most common and exact of them are the rigorous coupled-wave approach (RCWA) developed by Moharam and Gaylord [14, 15] and the modal approach [16, 17]. Both theories rely on the Floquet theorem and as such assume truly periodic structure of gratings. Coupled-wave method originates from the popular Kogelnik's coupled-wave (CW) theory [18]. It has been applied with success to different optical diffractive elements, first of all to analysis of the general planar-grating diffraction problem, and gave extremely accurate predictions for different orders of diffraction [19-28]. Method has been systematically extended to surface-relief dielectric gratings with different profiles: sinusoidal, square-wave, sawtooth, triangular, rectangular and others [20]. Modal approach also has its active development, including analytical and numerical methods [29-33]. Li proposed a multilayer modal method [30] in which a recursive and numerically stable S-matrix algorithm for modeling layered diffraction gratings has been developed.

The coupled-wave, modal and S-matrix methods are exact for the formulation but are numerical, and rather difficult, methods in the technique used to find solutions of the wave equation in the modulated region. Thus, the RCWA and S-matrix methods give rise to a not simple eigenvalue problem for the coefficient matrix constructed from the coupled-wave equations. On the other hand, the modal approach requires solving a transcendental equation – even more difficult computational problem. The convergence of these methods to the exact solutions of the original electromagnetic problem was proved mathematically [22], so the numerical results have the character of prediction rather than they are a subject of the strict and systematical verification by experiments. Most often they are used for testing of the approximate diffraction theories.

Currently there are various approximate versions of the rigorous coupled-wave and modal theories. Applying a series of fundamental assumptions to the rigorous theories, Gaylord and Moharam have obtained various approximate

diffraction theories for general case of sinusoidal permittivity planar dielectric grating [19]. Among them are the well known Kogelnik theory, Raman-Nath theory, closely related to it amplitude transmittance theory and others. Numerical results for diffraction efficiencies have been obtained and their good agreement with the results of rigorous theory was demonstrated in the appropriate limits. However, most of the approximate theories derived from the rigorous approaches still assume numerical solutions of the differential coupled wave equations and are primarily intended for bulk refractive index modulated planar sinusoidal gratings [33, 34]. At the same time, the most significant result of the rigorous theory is ascertainment of the fact that for obtaining accurate predictions of diffraction efficiency in the theory of transmission gratings more important is retention of higher-order waves in expansion of the electric field in space harmonics, than keeping boundary conditions and second derivatives of the field amplitudes [14]. And conversely, second derivatives and boundary diffraction are more important in case of reflection gratings, than inclusion of higher-order waves. This result may be useful for developing of an approximate theory from the very start. It is still interesting to find analytical expressions for the DE in order to study the different parameters influence in the efficiency of the different orders. Such program can be realized in thin grating approximation. The concept of "thin" refers not to the full thickness of the grating, but only to its physically deformed (modulated) region.

In this work the semi-analytical analysis of thin phase holographic gratings' efficiency is done using the method of spectral expansions for an infinite periodic lattice. Analytical dependences of the DE on parameters of lattices with arbitrary continuous profile, including sinusoidal one, is obtained. Surface-relief phase gratings are simply obtained through a well-known holographic PTP recording method. The used for calculations real samples of profile were obtained by Atomic Force Microscopy (AFM) measurement method. A satisfactory agreement between the numerical calculations and experimental measurements is demonstrated. The optimal profile shape is identified that provides the maximum efficiency.

## 2. Theoretical analysis of the diffraction efficiency of holographic gratings with arbitrary smooth relief

In this section we describe our theoretical analysis of the DE of thin phase holographic gratings. Thin phase screen (or mask) approximation [35, 36] is used, in which the modifications of light properties within the material are considered small and the grating is replaced by a thin screen that changes the local phase of the transmitted light. This phase modulation is taken into account by specifying the grating's deformation profile in the analytical form. The analysis is performed by using the method of spectral expansions for an infinite periodic lattice. The simplicity of the model allows obtaining analytical dependences of

the DE upon various parameters for lattices with arbitrary continuous profile, including sinusoidal one. On the basis of these dependences it is not only possible to quickly and effectively assess a particular result without to the use of cumbersome numerical calculations, but also to carry out the selection of optimal values of the parameters of the lattice to obtain maximum efficiency in a given diffraction order.

## 2.1 Method of spectral decomposition of electromagnetic field

We consider the diffraction of the plane wave

$$u(x, z) = A e^{ik_0(x \sin \alpha + z \cos \alpha)} \quad (2)$$

with amplitude  $A$  and wave vector  $\vec{k} = \{k_x, k_z\} = \{k_0 \sin \alpha, k_0 \cos \alpha\}$  on a one-dimensional periodic dielectric lattice with period  $d$ . The lattice lies in the plane  $z=0$ , and is directed along the axis  $X$ . The following notations are used:

$$k_0 = \frac{2\pi}{\lambda} \text{ - vacuum wave number,}$$

$\lambda$  - wavelength of light in vacuum,

$\alpha$  - angle of incidence.

$$u(x, z) = \sum_{m=-\infty}^{\infty} V_m(\Omega) \cdot \exp \left[ i \left( x(k_0 \sin \alpha + m\Omega) \pm z \sqrt{k_0^2 - (k_0 \sin \alpha + m\Omega)^2} \right) \right], \quad (5)$$

$$V_m(\Omega) = \frac{A}{d} \int_{-d/2}^{d/2} e^{ik_0(n-1)h(x)} \cdot e^{-im\Omega x} dx.$$

Here  $\Omega = 2\pi/d$  is the spatial frequency of the grating. When light propagates in the positive direction of the  $z$  axis in the exponent should be left the sign "+".

The resulting representation of the diffracted field (5) contains a full description of the analytical form of angular dispersion, as mathematically is the expansion in the full set of plane waves with spatial frequencies  $k_x = k_0 \sin \mathcal{G} = (k_0 \sin \alpha + m\Omega)$  and

$$k_z = k_0 \cos \mathcal{G} = \sqrt{k_0^2 - (k_0 \sin \alpha + m\Omega)^2}.$$

These waves correspond to different diffraction orders  $m$ . Here  $\mathcal{G}$  is the angle of diffraction and the term  $m\Omega$  describes the presence of a constant phase shift between adjacent lattice periods. The first of these two expressions determines the angles of diffraction peaks; it implies the well-known lattice equation:  $d(\sin \mathcal{G} - \sin \alpha) = m\lambda$ . From the second relation we can see that for  $(k_0 \sin \alpha + m\Omega)^2 \leq k_0^2$  we have the going to infinity homogeneous wave, and for  $(k_0 \sin \alpha + m\Omega)^2 > k_0^2$  - inhomogeneous, exponentially decaying with  $z > 0$ , waves (evanescent waves).

Representing the first of these conditions in the form of inequality of second degree in  $m$

In the model of a thin phase screen [35] the grating is described by its transmittance function (phase function of the lattice), which can be expressed as

$$t(x) = e^{ik_0(n-1)h(x)}, \quad (3)$$

where  $n$  is the refractive index of the lattice material (for a dielectric  $n = \varepsilon^{1/2}$ ,  $\varepsilon$  - dielectric constant),  $h(x)$  is a periodic in  $X$  function describing its profile (thickness variations).

In accordance with the accepted model the field, directly behind the grating, can be written in the form

$$u(x, z = +0) = u(x, z = -0) \cdot t(x) = A \exp[ik_0(x \sin \alpha + (n-1)h(x))] \equiv u(x, 0). \quad (4)$$

In the framework of the scalar theory of diffraction and applying the standard method of spectral decompositions (for example, see [37, 38]) the general expression for the diffracted in the region  $z > 0$  field can be written as:

$$\left( \frac{\lambda}{d} \right)^2 \cdot m^2 + 2 \frac{\lambda}{d} \sin \alpha \cdot m - \cos^2 \alpha \equiv f(m) \leq 0 \quad (6)$$

and determining its roots:

$$m_{1,2} = \frac{d}{\lambda} (\pm 1 - \sin \alpha) \quad (7)$$

we obtain the conditions of existence of propagating diffraction modes:  $m_2 \leq m \leq m_1$ , or explicitly:

$$-\frac{d}{\lambda} (1 + \sin \alpha) \leq m \leq \frac{d}{\lambda} (1 - \sin \alpha) \quad (8)$$

Analyzing the condition (8), we can see that for an arbitrary angle of incidence the defined by it regions of existence of positive and negative diffraction orders  $m = \pm 1, \dots$  are not symmetrical relative to zero-mode  $m = 0$  propagation direction (the direction by the angle of incidence  $\alpha \neq 0$ ). For example, at  $d = \lambda$  and positive  $\alpha$ , there exists only negative first-order mode  $m = -1$ , and vice versa, at  $d = \lambda$  and  $\alpha < 0$  observing is the positive mode  $m = +1$ .

## 2.2 Intensity distribution in the diffraction modes

According to the decomposition (5), the intensity of the diffracted field is the sum over the intensities  $I_m(\Omega)$  of each diffraction order  $m$ :

$$|u(x, z)|^2 = \sum_{m=-\infty}^{\infty} I_m(\Omega) = \sum_{m=-\infty}^{\infty} |V_m(\Omega)|^2. \quad (9)$$

Since there is no loss of energy in the phase optical element, the amount of decaying wave intensity in (9) describes the energy stored in the form of reactive power (energy of evanescent waves). Along with the distribution of the diffraction efficiency  $|V_m(\Omega)|^2$  in each order  $m$ , an important characteristic of the grating quality is the integral value of the energy-wise efficiency  $E_0$ , the corresponding fraction of energy per all diffraction orders [38]:

$$E_0 = \sum_{m=-M_1}^{-1} I_m + \sum_{m=1}^{M_2} I_m. \quad (10)$$

The maximum numbers  $M_1$  and  $M_2$  are orders of diffracted homogeneous waves in (9) that are determined from (8).

We did not use the explicit form of the transfer function  $t(x)$  of grating (3) in the derivation of the expansion (5). Thus, the representation, obtained for the diffracted by a one-dimensional periodic lattice field, is an exact solution, provided that the field  $u(x, 0)$  is known in the plane of the lattice. For the specific intensity calculations the explicit form of the profile function  $h(x)$  must be given.

Further, we first derive the formulas for a pure sinusoidal phase grating, and then consider the lattice with real profiles obtained by the AFM.

## 2.3 Sinusoidal phase grating

For a grating with a sinusoidal profile the grating function  $h(x)$  in (5) can be written in the form

$$h(x) = l_0 + \frac{h_0}{2} + \frac{h_0}{2} \cos \Omega x, \quad (11)$$

where  $l_0$  is the thickness of unmodulated part of the layer,

$h_0$  is the depth of modulation,

$\Omega = 2\pi/d$  is the spatial frequency of the grating,

$d$  is the grating (fringe) period.

Substituting (11) for the profile function in (5) for the spectral coefficients  $V_m(\Omega)$  and making the necessary integration with the well-known Jacobi - Anger expansion on cylindrical functions [37, 39]

$$e^{ix \cos \varphi} = J_0(x) + 2 \sum_{n=1}^{\infty} i^n J_n(x) \cos(n\varphi) \quad (12)$$

we obtain:

$$V_m(\Omega) = A e^{i(n-1)k_0(l_0+h_0/2)} \cdot i^m J_m(\beta), \quad (13)$$

where  $\beta = (n-1)k_0 h_0 / 2 = \pi(n-1)h_0 / \lambda$ . Thus, for a sinusoidal phase grating the intensity distribution in the diffraction orders  $m$  is expressed by the square of the Bessel functions

$$I_m = |V_m(\Omega)|^2 = [A \cdot J_m(\beta)]^2. \quad (14)$$

As the sum of the squared Bessel functions over all orders  $m$  is unity

$$\sum_{m=-\infty}^{\infty} J_m^2(\beta) = 1,$$

the expression (14) conserves the input power of light.

As one can see, the diffraction efficiency is determined by two parameters: the refractive index  $n$  and the ratio of the modulation depth  $h_0$  to the incident wavelength  $\lambda$ . The unmodulated part  $l_0$  of thickness is not included in the expression for the intensity. As the determining thickness factor acts only the peak-to-trough height  $h_0$  of the grating profile. The grating period  $d$  is not included as well. This is due to the fact that the coefficients  $V_m$  in the expansion (5) are normalized to  $d$  coefficients of the Fourier expansion for periodic with respect to  $d$  function  $\exp[ik_0(n-1)h(x)]$  (see (11)) in the plane waves with spatial frequencies  $m\Omega = 2\pi m/d$ . The result (14) is consistent with that of Raman-Nath theory obtained for the case of an unslanted fringe transmission grating [19]:  $\eta_m = J_m^2(\pi \varepsilon_1 h_0 / \lambda \cos \vartheta)$ , where  $\varepsilon_1$  is the amplitude of the sinusoidal relative permittivity,  $\vartheta$  is the angle of refraction of the incident wave. Differences are only in the details of grating's model (in the description of the phase difference). So we can conclude that 'thin' grating in our case is the same as 'thin' grating that produces Raman-Nath diffraction regim in planar case [40].

## 2.4 Periodic lattice with an arbitrary profile

In the expression (5) for the spectral coefficients  $V_m(\Omega)$ , we consider now the profile function of general form. On the lattice period  $-d/2 \leq x \leq d/2$  we approximate it with the B-spline first-order polynomials

$$h_j(t) = h_j + (h_{j+1} - h_j) \cdot t, \quad t \in [0, 1] \quad (15)$$

where  $h_j$  are samples  $h(x)$  defined at discrete

points  $j = 0, 1, \dots, N-1$ ,

$\delta = d/N$  is the sampling step,

$N$  is the number of partition segments.

Now the integral  $V_m(\Omega)$  in (5) is splitting into sum of integrals over the intervals of the period  $d$  partition. Omitting the details of calculations, we give the result of the integration

$$V_m(\Omega) = \frac{A}{N} \sum_{j=1}^N \operatorname{sinc}\left(\frac{\beta_j d}{2N}\right) \cdot \exp\left[i\left(\alpha_j + (2j-1-N)\frac{\beta_j d}{2N}\right)\right], \quad (16)$$

were

$$\operatorname{sinc}(x) = \sin x / x, \quad \alpha_j = h_j k_0 (n-1),$$

$$\beta_j = (h_{j+1} - h_j) k_0 (n-1) - m\Omega, \quad \Omega = 2\pi / \alpha.$$

Expressing the exponent in (16) in terms of trigonometric functions, we obtain the final expression for the intensity distribution in diffraction orders:

$$I_m = |V_m(\Omega)|^2 = \left(\frac{A}{N}\right)^2 \left\{ \left[ \sum_{j=1}^N \operatorname{sinc}\left(\frac{\beta_j d}{2N}\right) \cdot \cos\left[\alpha_j + (2j-1-N)\frac{\beta_j d}{2N}\right] \right]^2 + \left[ \sum_{j=1}^N \operatorname{sinc}\left(\frac{\beta_j d}{2N}\right) \cdot \sin\left[\alpha_j + (2j-1-N)\frac{\beta_j d}{2N}\right] \right]^2 \right\}. \quad (17)$$

The number of points  $N$  per grating's period used in numerical calculations by this formula was taken equal to the number of samples in AFM profile measurements and for different examples was of 45-55 points per period.

### 3. Numerical analysis of the diffraction mode intensities

In this section, we consider some examples of calculation according to the above formulas of the intensities in different diffraction orders. We assume a normally incident plane wave of unit amplitude at the wavelength  $\lambda = 0.63 \mu\text{m}$ . The modulation depth  $h_0$  of profile in all examples is less than the wavelength (thin grating). The periodic lattice has an arbitrary continuous profile, and the conditions of existence of the homogeneous waves  $m = -1, 0, 1$  are satisfied.

#### 3.1 Simple sinusoidal phase grating

Calculations are performed using the formula  $I_m = [J_m(\beta)]^2$ ,  $\beta = \pi(n-1)h_0/\lambda$  for  $m = -1, 0$  and formula (10) for energy-wise efficiency  $E_0$ . Fig. 1 represents the dependence of diffraction intensities (in percent) upon the depth of profile  $h_0$  for a fixed value  $\varepsilon = 3.0$ , typical for thermo-plastic polymer layers. There are three specific points  $h_0$  in which, respectively:

$$1. I_{-1}(h_0) = I_0(h_0) = 29.98\%, \quad h_0 = 0.39 \mu\text{m} \approx 0.6\lambda.$$

Equal intensities in orders  $\pm 1$  and 0. The energy-wise efficiency of the grating  $E_0 \approx 60\%$ . Minimal loss of intensity in heterogeneous diffraction orders. For given values of the parameters the grating can be used as a beam splitter. The next points  $h_0$  of intensity intersection on the chart yield smaller efficiency;

$$2. I_{-1}(h_0) = 33.86\%, \quad I_0(h_0) = 9.94\%, \quad h_0 = 0.51 \mu\text{m} \approx 0.8\lambda.$$

The maximum theoretically possible value for the intensity  $I_{-1}(h_0)$  of sinusoidal grating. Energy-wise efficiency also has its maximum  $E_0 \approx 68\%$ . For a given depth of modulation grating can be used as a beams deflector;

$$3. I_{-1}(h_0) = 26.93\%, \quad I_0(h_0) = 0.00\%, \quad h_0 = 0.66 \mu\text{m} \approx 1.0\lambda.$$

The lack of intensity in the zero order  $I_0(h_0) = 0$ . Energy-wise efficiency is  $E_0 \approx 54\%$ .

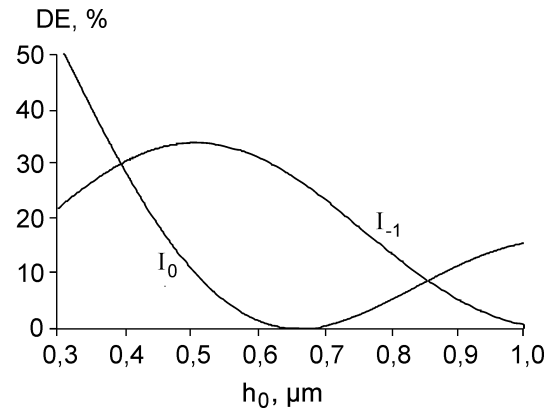


Fig. 1. Dependences of the diffraction efficiency of sinusoidal grating in the zero and first diffraction orders upon modulation depth  $h_0$ .

A further increase of profile depth at fixed value of the dielectric constant  $\varepsilon$  decreases the values of diffraction intensity. As  $\varepsilon$  is a part of the Bessel function argument in the form of the factor  $(\varepsilon^{1/2} - 1) \cdot h_0$  (see (13)), the dependence family of the intensity on  $h_0$  at smaller  $\varepsilon$  maintains its character, systematically shifting to the left.

#### 3.2 Grating with measured by AFM arbitrary profile

The creation of a grating with an ideal sinusoidal profile is possible provided a weak linear deformation of the thermoplastic layer. In reality, however, to increase efficiency, the depth of modulation must be increased, which naturally leads to the nonlinear deformation and to the deviation from the sinusoidal form. Thus, the real profile, obtained by nonlinear recording, can be established only by direct measurements, such as the AFM profile measurements.

Fig. 2 shows the result of such a measurement of a quasi-sinusoidal grating. We can see that the measured

profile has irregular character both in the form and in the depth of modulation. This is primarily due to the imperfect character of the recorded grating but also due to the nature of geometrical shape measurements performed with the AFM.

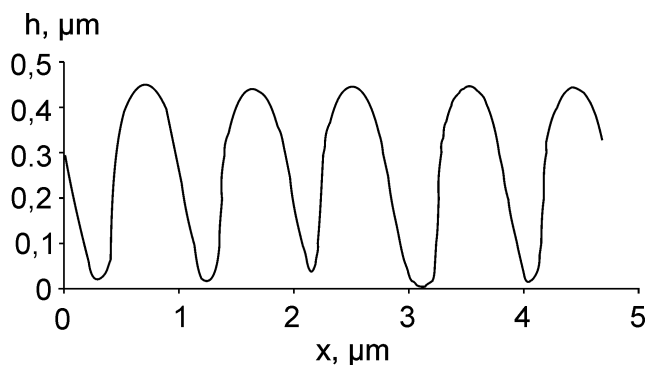


Fig. 2. A sample of AFM measured quasi-sinusoidal profile with  $d \approx 0.95\mu\text{m}$ ,  $h_0 \approx 0.44\mu\text{m}$ .

A characteristic feature of the AFM measurements is that the graphs of narrow and deep profiles are asymmetric (have a systematic tilt towards the cantilever move direction) due to the finite cantilever dimensions. In this case, we have to either artificially reconstruct the symmetry of curve in Fig. 2 or assess the energy-wise efficiency as the sum (10) over the intensities in the first orders of diffraction  $E_0 = I_1 + I_{-1}$ . Under the conditions of imperfect data, the characteristic  $E_0$  is more presentational. In the following examples of calculations both approaches are used.

**Example 1.** The grating with quasi-sinusoidal profile,  $d \approx 0.95\mu\text{m}$ ,  $h_0 \approx 0.44\mu\text{m}$  (Fig. 2). Fig. 3 presents the dependence of values  $E_0, I_1, I_{-1}$  on the dielectric constant  $\varepsilon$  taken in the range of 2-5 and calculated for a grating with measured profile of 4-th groove. The maximum of  $E_0$  equals to 68.9 at  $\varepsilon = 3.3$  ( $n = 1.82$ ). This value is very close to the value of  $\varepsilon$  for used thermoplastic material. So, in the real case of symmetrical grooves the  $I_{-1}$  and  $I_1$  can be estimated to the value of 34.5. Numerical symmetrization of groove's profile gives somewhat lower values:  $E_0 = 63.0$ ,  $I_{-1} = I_1 = 31.5$ . Thus, the results are closer to those of pure sinusoidal grating.

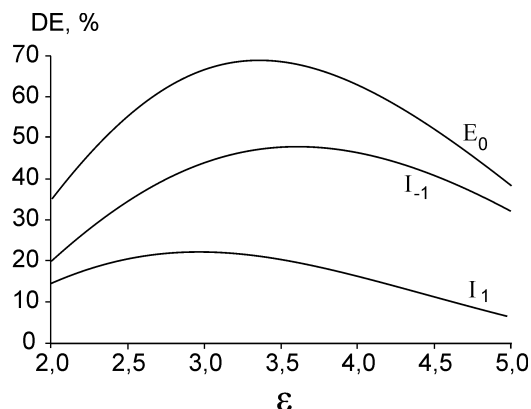


Fig. 3. Diffraction efficiency for real form of 4-th groove in Fig. 2. Maximum values:  $E_0 = 68.91$ ,  $\varepsilon = 3.3$  ( $n = 1.82$ );  $I_{-1} = 48.08$ ,  $\varepsilon = 3.6$  ( $n = 1.90$ );  $I_1 = 22.62$ ,  $\varepsilon = 3.0$  ( $n = 1.73$ ).

This example shows that for the real asymmetric profiles the obtained values of the diffraction efficiency in one of the diffraction orders can be much higher than the limit value for the sinusoidal grating. This obviously means that the holographic gratings with asymmetric profile exhibit blazing characteristics. The only limitation is the possibility of practical realization of the desired profile. An universal fabrication method for holographic blazed gratings based on Fourier exposure synthesis has been proposed in [41].

**Example 2.** A sample of grating with measured profile,  $d \approx 0.96\mu\text{m}$ ,  $h_0 \approx 0.42\mu\text{m}$ . A characteristic feature of this example is the presence of a small shelf in the minima of the grating profile (Fig. 4). The rough edges suggest that a tearing apart of the thermo-plastic material in the valleys has occurred as a result of the strong influence of electrostatic forces. The calculations were made for the second groove. In the Figure 5 the dependences of  $E_0, I_{-1}, I_1$  on  $\varepsilon$  are presented.

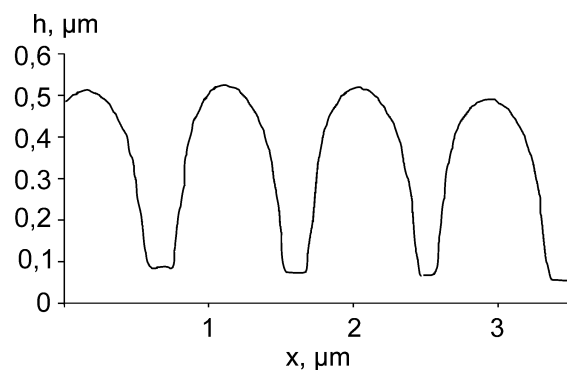


Fig. 4. A sample of AFM measured profile with the presence of small shelves in the minima  $d \approx 0.96\mu\text{m}$ ,  $h_0 \approx 0.42\mu\text{m}$ .

The maximum value of  $E_0$  equals to 63.7 at  $\varepsilon = 3.2$  ( $n = 1.79$ ). The curves  $I_{-1}$  and  $I_1$  are similar in form and in values, which is the result of a higher symmetry of grooves than in the case of grating in Figure 2. The maximum efficiency  $E_0$ , obtained in this example, is smaller than that in the Example 2. A possible explanation for this is that the modulation depth of the thermoplastic deformation in the first example is larger (cf. Figs. 2 and 4).

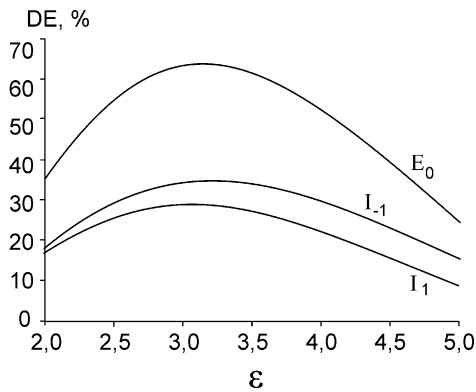


Fig. 5. Diffraction efficiency for measured form of the second groove in Fig. 4. Maximum values:  $E_0 = 63.70$ ,  $\varepsilon = 3.2$  ( $n = 1.79$ );  $I_{-1} = 34.89$ ,  $\varepsilon = 3.2$  ( $n = 1.79$ );  $I_1 = 28.95$ ,  $\varepsilon = 3.1$  ( $n = 1.76$ ).

**Example 3.** A sample of grating of measured profile with  $d \approx 0.98\mu\text{m}$ ,  $h_0 \approx 0.41\mu\text{m}$ . It is an example, when the electrostatic forces were strong enough during deformation to force all of the thermo-plastic material into the ridges, leaving the underlying photoconductor layer exposed (Figure 6). The calculations were made for the second groove. The dependences of  $E_0$ ,  $I_{-1}$ ,  $I_1$  on  $\varepsilon$  are presented in Figure 7. The maximum value of  $E_0$  equals to 76.2 at  $\varepsilon = 3.4$  ( $n = 1.84$ ). Curves  $I_{-1}$  and  $I_1$  are very different from each other, since the symmetry of the measured profile is strongly distorted. The maximum mean value of intensities  $I_{-1}$  and  $I_1$  is thus 38.1, which is in good agreement with our experimental data.

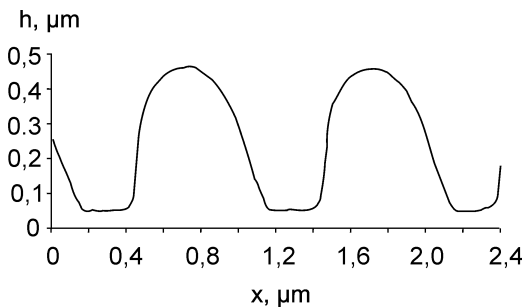


Fig. 6. The profile with  $d \approx 0.98\mu\text{m}$ ,  $h_0 \approx 0.41\mu\text{m}$ , obtained under strong electrostatic impact.

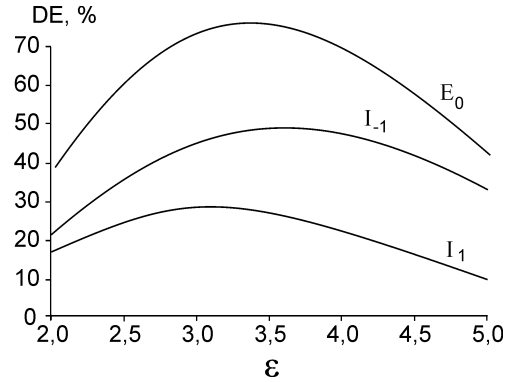


Fig. 7. Diffraction efficiency for the measured form of 1-st groove in Fig. 6. Maximum values:  $E_0 = 76.23$ ,  $\varepsilon = 3.4$  ( $n = 1.84$ );  $I_{-1} = 49.04$ ,  $\varepsilon = 3.6$  ( $n = 1.90$ );  $I_1 = 28.40$ ,  $\varepsilon = 3.1$  ( $n = 1.76$ ).

The developed method of the numerical analysis of DE can be easily applied in numerical experiments aimed to find the optimal shape for the profile, giving maximum efficiency in certain orders. Successive variation of the grating profile shape (shown in the third example) has shown that the desired shape (Fig. 8) resembles to that of a binary grating with equal sizes of open and closed sections of the period  $a = b = d/2$ .

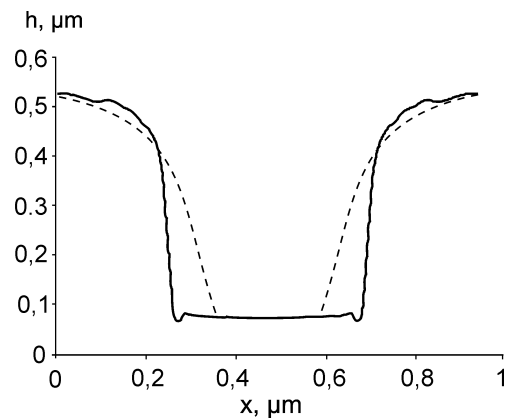


Fig. 8. Optimized groove form providing the maximum DE.

The grating efficiency with such a profile tends to its limiting value of 40.5 (theoretical value of efficiency maximum for the binary rectangular lattice [3]). So, the grating with those in Fig. 8 profile (marked by the thick line) has a calculated efficiency of  $I_{-1} = 39.98$  at  $\varepsilon = 3.0$  ( $n = 1.73$ ). The dependences of  $E_0$ ,  $I_{-1}$ ,  $I_1$  on  $\varepsilon$  are presented in the Fig. 9. We conclude thus that at normal incidence the value of 40.5 for efficiency is the limiting one for any smooth profile of symmetrical shape.

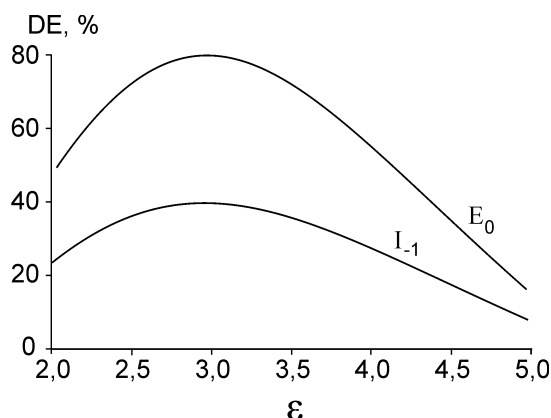


Fig. 9. Diffraction efficiency for optimal shape shown in Fig. 8.  $DE_{\max}: E_0 = 79.94, I_{-1} = I_1 = 39.98, \varepsilon = 3.01$  ( $n = 1.73$ ).

#### 4. Conclusion

Developed in this paper method of numerical analysis of the DE of holographic diffraction gratings with arbitrary continuous profile has confirmed the known results for gratings with a sinusoidal profile. Approach of thin grating in our case is the same as in the Raman-Nath approach for planar sinusoidal gratings. Method enables to determine the shape of a non-sinusoidal symmetric profile for which the maximum value of efficiency is achieved. The shape of the profile and the DE value tend to those for the binary rectangular grating with equal sizes of open and closed sections of the period  $a = b = d/2$  and with the DE = 40.5% at normal incidence. In the case of a non-symmetric smooth profile efficiencies in the first plus- and minus-orders can differ greatly. This result qualitatively is in agreement with the case of slanted Bragg planar grating. It means that the holographic gratings with asymmetric profile exhibit blazing characteristics. It is not difficult to obtain numerically the asymmetric profiles with values of DE in one of the diffraction order much higher than the limit value for the sinusoidal grating. The only limitation is the possibility of practical creation of the desired profile. The obtained satisfactory agreement of numerical results with the experimental data confirms the conclusion of the rigorous theory that in case of transmission gratings more important is retention of higher-order waves than keeping boundary conditions and second derivatives of the field amplitudes [14].

The simplicity of the described model allows obtaining analytical dependences of the diffraction efficiency on various parameters for lattices with arbitrary continuous profile, including sinusoidal one. On the basis of these dependences it is not only possible to quickly and effectively assess a particular result without using cumbersome numerical calculations, but also to choose optimal values of the parameters of the lattice to obtain maximum efficiency in a given diffraction order.

#### Acknowledgments

This research was partially supported by the Science and Technology Center in Ukraine (STCU Project nr. 5808) and the Academy of Sciences of Moldova (Project nr. 15.817.02.38A).

#### References

- [1] R. Petit, *Electromagnetic Theory of Gratings*, Springer-Verlag, Berlin, (1980).
- [2] R. J. Collier, *Optical Holography*, Academic Press, (1971).
- [3] C. Palmer, *Diffraction Grating Handbook*, 5th Edition, Thermo RGL Rochester, New York, (2002), <http://www.gratinglab.com/library/handbook5/handbook.asp>
- [4] T. L. Credelle, F. W. Spong, in *Selected Papers on Holographic Recording Materials*, Ed. Hans I. Bjelkhagen, SPIE milestone series, p. 619, 1996.
- [5] *Selected Papers on Holographic Recording Materials*, Ed. Hans I. Bjelkhagen, SPIE milestone series, V. MS 130, 1996.
- [6] U. Schnars, W. Jüptner, *Meas. Sci. Technol.* **13**, 85 (2002).
- [7] S. V. Gurevich, V. B. Konstantinov, E. V. Konstantinova, L. G. Malkhasyan, A. F. Malyi, V. F. Relyn, *Real-Time Holographic Interferometry and Optical Data Processing in Physical Experiments*, <http://www.ioffe.ru/PAPERS/97w08.pdf>
- [8] K. Munakata, K. Harada, H. Anji, M. Itoh, T. Yatagai, S. Umegaki, *Optics Letters* **26**(1), 4 (2001).
- [9] L. M. Panasyuk, A. M. Nastas, *Optics and Spectroscopy Journal* **94** (6), 959 (2003).
- [10] A. Chirita, N. Kukhtarev, T. Kukhtareva, O. Korshak, V. Prilepov, Yu. Jidcov, *J. Mod. Opt.* **59**(16), 1428 (2012).
- [11] A. Chirita, F. Dimov, S. Pradhan, P. Bumacod, O. Korshak, *Journal of Nanoelectronics and Optoelectronics* **7**(5), 415 (2012).
- [12] A. Chirita, N. Kukhtarev, O. Korshak, V. Prilepov, Yu. Jidcov, *Laser Physics* **23**, 036002-6 (2013).
- [13] A. Chirita, T. Galstean, M. Caraman, O. Korshak, V. Prilepov, I. Andries, *J. Optoelectron. Adv. Mater.* **7**(3-4), 293 (2013).
- [14] M. G. Moharam, T. K. Gaylord, *J. Opt. Soc. Am.* **71**, 811 (1981).
- [15] M. G. Moharam, T. K. Gaylord, *J. Opt. Soc. Am.* **73**(9), 1105 (1983).
- [16] S. T. Peng, T. Tamir, H. L. Bertoni, *IEEE Trans. Microwave Theory Tech. MTT-23*, 123 (1975).
- [17] R. S. Chu, J. A. Kong, *IEEE Trans. Microwave Theory Tech. MTT-25*, 18 (1977).
- [18] H. Kogelnik, *Bell Syst. Tech. J.* **48**, 2909 (1969).
- [19] T. K. Gaylord, M. G. Moharam, *Applied Physics B* **27**, 1 (1982).
- [20] M. G. Moharam, T. K. Gaylord, *J. Opt. Soc. Am.* **72**, 1385 (1982).

- [21] T. K. Gaylord, M. G. Moharam, *Proc. IEE.* **73**, 894 (1895).
- [22] M. G. Moharam, E. B. Grann, D. A. Pomet, T. K. Gaylord, *J. Opt. Soc. Am. A* **12**, 1068 (1995).
- [23] M. G. Moharam, T. K. Gaylord, *J. Opt. Soc. Am. A* **3**, 1780 (1986).
- [24] N. Kamiya, *Appl. Opt.* **37**, 5843 (1998).
- [25] P. Dansas, N. Paraire, *J. Opt. Soc. Am. A* **15**, 1586 (1998).
- [26] N. Y. Chang, C. J. Juo, *J. Opt. Soc. Am. A* **18**, 2491 (2001).
- [27] W. H. Southwell, *J. Opt. Soc. Am. A* **5**, 1558 (1998).
- [28] P.-A. Blanche, P. Gailly, S. Habraken, P. Lemaire, C. Jamar, *Opt. Eng.* **43**(11), 2603 (2004).
- [29] D. M. Pai, K. A. Awada, *J. Opt. Soc. Am. A* **8**, 755 (1991).
- [30] L. J. Li, *Opt. Soc. Am. A* **10**, 2581 (1993).
- [31] L. J. Li, *Opt. Soc. Am. A* **11**, 2829 (1994).
- [32] I. Yaremchuk, T. Tamulevičius, V. Fitio, I. Gražulevičiūtė, Y. Bobitski, S. Tamulevičius, *J. Mod. Opt.* **60**(20), 1781 (2013), <http://dx.doi.org/10.1080/09500340.2013.861032>
- [33] D. Song, Y. Y. Lu, *J. Mod. Opt.* **60**(20), 1729 (2013), <http://dx.doi.org/10.1080/09500340.2013.856484>
- [34] L. Estepa, C. Neipp, J. Frances, A. Marquez, S. Bleda, M. Pérez-Molina, M. Ortuño, S. Gallego, *Proc. of SPIE.* 8171, 81710R-1, (2011).
- [35] A. Goncharskiy, V. Popov, V. Stepanov, *Introduction to Computer Optics: Textbook*; MSU: Moscow (1991), (in Russian).
- [36] A. Ishimaru, *Wave Propagation and Scattering in Random Media*; Academic Press: NY (1978).
- [37] S. Solimeno, B. Crosignani, P. DiPorto, *Guiding, Diffraction and Confinement of Optical Radiation*; Academic Press, Inc. (1986).
- [38] *Methods for Computer Design of Diffractive Optical Elements*, Ed. V. A. Soifer, Wiley: New York (2002).
- [39] A. Erdelyi, *Higher Transcendental Functions, Volume 2*; Dover Publications (2007).
- [40] T. K. Gaylord and M. G. Moharam, *Appl. Opt.* **20**, 3271 (1981).
- [41] J. Ling, D. Zhang, Y. Huang, Q. Wang, S. Zhuang, *J. Mod. Opt.*, **61**(2), 132 (2014), <http://dx.doi.org/10.1080/09500340.2013.871362>

---

\*Corresponding author: iandriesh@mail.ru